Adaptive Multiplexing Order Selection For Single-carrier MIMO Transmission

Ryo NAGAOKA† Shinya KUMAGAI† Tetsuya YAMAMOTO† and Fumiyuki ADACHI‡

†‡ Dept. of Communications Engineering, Graduate School of Engineering, Tohoku University
6-6-05, Aza-Aoba, Aramaki, Aoba-ku, Sendai, Miyagi, 980-8579, Japan
E-mail: †{nagaoka, kumagai, yamamoto}@mobile.ecei.tohoku.ac.jp, ‡adachi@ecei.tohoku.ac.jp

Abstract— **Spatial multiplexing and diversity are in a tradeoff relationship. Multiple-input multiple-output (MIMO) can increase the maximum throughput in a good propagation environment by selecting high multiplexing order, but the achievable throughput degrades in a poor propagation environment. By adaptively selecting the multiplexing order according to the changing propagation environment, the achievable throughput can always be maximized. In this paper, we consider single-carrier (SC)-MIMO with frequency-domain equalization (FDE) and propose an adaptive multiplexing order selection suitable for the cyclic delay pilot channel estimation (CDP-CE). The throughput performance achievable with the SC-MIMO adaptive multiplexing order selection in a multi-cell environment is evaluated by computer simulation.**

Keywords-MIMO, STTD, SDM multiplexing order, diversity order, multi-cell environment

I. INTRODUCTION

The broadband wireless channel is characterized by path loss, shadowing loss, and frequency-selective fading [1]. In a cellular network, the same frequency is reused in spatially separated cells to efficiently utilize the limited frequency bandwidth. Therefore, as the mobile terminal (MT) approaches the cell edge, the received signal power degrades and furthermore, the co-channel interference (CCI) from neighboring cells gets stronger. The received signal-to-interference plus noise power ratio (SINR) drops near the cell edge. On the other hand, users near the cell center can enjoy high SINR. To achieve the best throughput always in a changing SINR environment, the use of multiple transmit and receive antennas known as multiple-input multiple-output (MIMO) [2] is effective.

There is a trade-off relationship between the spatial multiplexing and diversity in MIMO [2, 3]. An extreme case is the full-order diversity for transmitting the single-stream (the spatial multiplexing order Z is one). The full-order diversity aims at maximizing the received SINR and hence, can improve the SINR of a user at the cell edge. The spatial diversity using orthogonal space-time block code (STBC) achieves the full-order diversity with low computational complexity [4]. Another extreme case is the full-order spatial multiplexing known as space division multiplexing (SDM) [5]. The same number of data streams as the number of transmit antennas can be simultaneously transmitted (of course, at least, the number of receive antennas must be equal or higher than that of transmit antennas). This can be applied for a user near the cell center where high SINR is obtained. For achieving always the best throughput according to the changes in the received SINR, the multiplexing order needs to be adaptively selected.

Simple switching between full spatial diversity and full spatial multiplexing was studied in [6-8]. However, adaptive multiplexing order selection has not been fully studied yet. How the adaptive multiplexing order selection improves the throughput performance in a cellular network has not been fully investigated.

In this paper, we consider an uplink transmission using single-carrier (SC)-MIMO with frequency-domain equalization (FDE) [9, 10] and propose an adaptive multiplexing order selection. The multiplexing order is determined based on maximum throughput criterion. For the transmission of single data stream, the space-time block coded transmit diversity (STTD) with FDE (FD-STTD) [11] is assumed. STTD can get the full-order diversity gain. For the transmission of multiple data streams, SDM with minimum mean square error based detection (MMSED) combined with FDE (FD-SDM) [12] is used. FDE requires the knowledge of channel state information (CSI) and CCI plus noise power. Both of FD-STTD and FD-SDM do not require the CSI at the MT transmitter while requiring the CSI at the base station (BS) receiver. Therefore, the complexity problem at the MT transmitter can be alleviated. As for the channel estimation, we apply the MIMO cyclic delay pilot channel estimation (CDP-CE) [13]. The proposed an adaptive multiplexing order selection is suitable for CDP-CE.

The remainder of this paper is organized as follows. Sect. II presents the SC-MIMO uplink transmission model. In Sect. III, the proposed adaptive multiplexing order selection suitable for CDP-CE is described. In Sect. IV, the SC-MIMO throughput performance achievable with the proposed adaptive multiplexing order selection in a multi-cell environment is evaluated by computer simulation. Sect. V offers some concluding remarks.

II. SC-MIMO UPLINK TRANSMISSION MODEL

A. Uplink model

In a cellar network, available bandwidth is divided into F and assigned to each cell. This index F is called cluster size. The bandwidth allocated to each cell becomes wider as F is gets smaller, but the impact of CCI gets stronger.

The SC-MIMO uplink model considered in this paper is shown in Fig. 1. The central cell (c=0) is the cell of interest and there are 6 CCI cells in the first tier that use the same frequency, and CCI cells far from the first tier cells are assumed to be negligible because their CCIs are too small. It is supposed that an MT having N_t transmit antennas is located randomly in each cell. It is assumed a BS with N_r receive antennas is located at the center of each cell.

B. Propagation channel model

The broadband channel is featured by distance-dependent path loss, log normally distributed shadowing loss, and frequency-selective fading. Under the frequency-selective fading channel which consists of L discrete paths, the channel impulse response between the n_t-th transmit antenna and the n_r-th receive antenna in the c-th cell is given as

$$h^{(c)}_{n_r,n_t}(\tau)=\sum_{l=0}^{L-1} h^{(c,l)}_{n_r,n_t}\cdot\delta(\tau-\tau^{(c,l)}_{n_r,n_t})\ , \tag{1}$$

where

$$h^{(c,l)}_{n_r,n_t}=\sqrt{r_c^{-\alpha}\cdot 10^{-\eta_c/10}}\cdot g^{(c,l)}_{n_r,n_t}\ , \tag{2}$$

with r_c, η_c , and α being the distance between MT in the c-th cell and BS in the 0-th cell, shadowing loss in dB having zero-mean and standard deviation σ_s, and path loss exponent, respectively. $g^{(c,l)}_{n_r,n_t}$ and $\tau^{(c,l)}_{n_r,n_t}$ are the complex-valued pass gain and the delay time of the l-th path between the n_t-th transmit antenna of MT in the c-th cell and the n_r-th receive antenna of BS in the 0-th cell. We assume $E\left[\sum_{l=0}^{L-1}\left|g^{(c,l)}_{n_r,n_t}\right|^2\right]=1$. The average received signal power $\Phi_r^{(c,n_t)}$ from n_t-th transmit antenna in the c-th cell is expressed as

$$\Phi_r^{(c,n_t)}=\Phi_t^{(c,n_t)}\cdot r_c^{-\alpha}\ , \tag{3}$$

where $\Phi_t^{(c,n_t)}$ is the transmit power of the n_t-th transmit antenna in the c-th cell and r_c is the distance between MT and BS in the c-th cell. By introducing the normalized distance r_c/R, where R is the cell radius, and the normalized transmit power $\phi_t^{(c,n_t)}=\Phi_t^{(c,n_t)}\cdot R^{-\alpha}$, Eq. (3) can be rewritten as

$$\Phi_r^{(c,n_t)}=\phi_t^{(c,n_t)}\cdot\left(r_c/R\right)^{-\alpha}. \tag{4}$$

We assumed that the transmit power is the same among all cells.

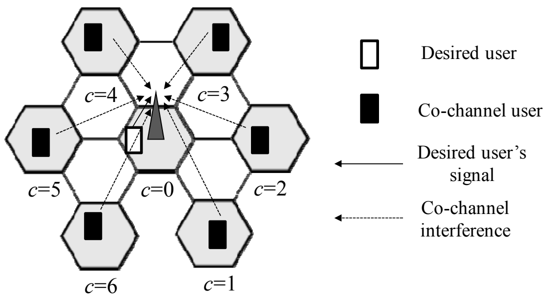

Fig. 1. SC-MIMO uplink model when F=3.

C. FD-STTD(Z=1)

SC-MIMO with N_t transmit antennas and N_r receive antennas is considered. Fig. 2 shows the transmission model of FD-STTD. 2 blocks with N_c data symbols are transformed by N_c-point fast Fourier transform (FFT) into the frequency-domain data symbol blocks and STBC is applied. The transmit signal blocks after the STBC encoding are transformed by N_c-point inverse FFT (IFFT) into the time-domain transmit signal blocks. The last N_g symbols of data symbol blocks with N_c symbols are copied as a cyclic prefix (CP) and inserted into the guard interval (GI) at the beginning of data symbol blocks to avoid the inter-block interference (IBI). After CP insertion, the transmit signal blocks are transmitted.

The received signal blocks after CP removal are transformed by N_c-point FFT into the frequency-domain received signal blocks. STBC decoding and FDE are applied to frequency-domain received signal blocks. The received blocks after decoding are transformed by N_c-point IFFT into the time-domain signal and received data sequence is obtained after demodulation.

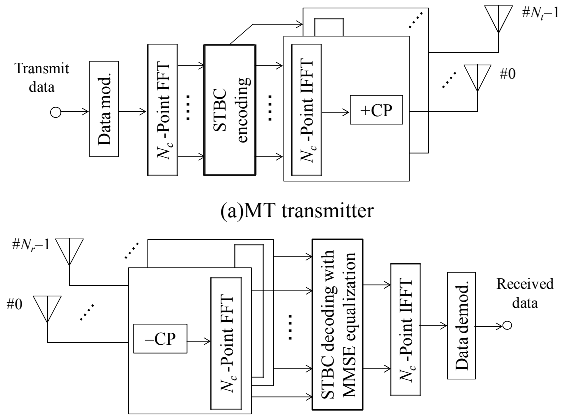

(a)MT transmitter

(b)BS receiver

Fig. 2. Transmitter/receiver for FD-STTD.

D. FD-SDM($Z\geq 2$)

Fig. 3 shows the transmission model of FD-SDM. Information bits are serial-to-parallel (S/P) converted to N_t information bit groups and data modulated. The symbols are transmitted with equal power by N_t antennas after CP insertion.

The signals are transmitted over a MIMO channel and received by N_r receive antennas. The received signal blocks after CP removal are transformed by N_c-point FFT into the frequency-domain received signal blocks. The MMSED combined with FDE is applied to frequency-domain received signal blocks. The received signal blocks after MMSED are transformed by N_c-point IFFT into the time-domain signal blocks. Then, the data-demodulated received signal blocks are parallel-to-serial (P/S) converted and received information bits are obtained.

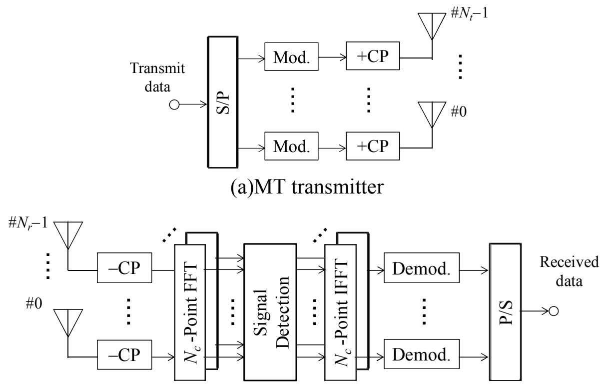

(a)MT transmitter

(b)BS receiver

Fig. 3. Transmitter/receiver for FD-SDM.

III. ADAPTIVE MULTIPLEXING ORDER SELECTION

The adaptive multiplexing order selection suitable for CDP-CE is proposed. First, we present the operation principle of CDP-CE and then, describe the proposed adaptive multiplexing order selection of Z=1~4 based on the maximum throughput criterion.

A. CDP-CE

Fig. 4 and Fig. 5 show the transmission model of CDP-CE and the frame structure. The pilot block having different cyclic delay is simultaneously transmitted from each transmit antenna, and hence, channel gain between all transmit and receive antennas can be simultaneously estimated. In this paper, N_d data blocks are transmitted after N_p pilot blocks in 1 frame from each transmit antenna.

The pilot block $\{p(t);t=0\sim N_c-1\}$ is added the different cyclic delay from each transmit antennas. The pilot block at the n_t-th transmit antenna is expressed as

$$p_{n_t}(t)=p((t-\Delta n_t)\bmod N_c),t=0\sim N_c-1\,, \tag{5}$$

where Δ is the cyclic delay amount satisfied $N_g\leq\Delta\leq N_c/N_t$. After CP insertion, the pilot symbol blocks are transmitted with equal power by N_t antennas.

The signals are transmitted over a MIMO channel and received by N_r antennas. The received signal blocks after CP removal are transformed by N_c-point FFT into the frequency-domain received signal blocks. The v-th pilot block at the n_r-th receive antenna in the k-th frequency is given as

$$R_{n_r}^{(v)}(k)=\sum_{t=0}^{N_t-1}H_{n_r,n_t}(k)\exp\left(-j\frac{2\pi k\Delta n_t}{N_c}t\right)P(k)\\+\Pi_{n_r}^{(v)}(k)+\Psi_{n_r}^{(v)}(k)\,, \tag{6}$$

where $P(k)$, $\Pi_{n_r}^{(v)}(k)$, and $\Psi_{n_r}^{(v)}(k)$ are the pilot block in the k-th frequency, additive white Gaussian noise having zero mean and variance $2\sigma_{noise}^2$, and CCI component, respectively. $H_{n_r,n_t}(k)$ is the channel transfer function including the transmit power between the n_t-th transmit antenna and n_r-th receive antenna in 0-th cell, and given as

$$H_{n_r,n_t}(k)=\frac{1}{\sqrt{N_t}}\sqrt{\frac{2E_s}{T_s}}\sum_{l=0}^{L-1}h_{n_r,n_t}^{(0,l)}\exp\left(-j2\pi k\frac{\tau_{n_r,n_t}^{(0,l)}}{N_c}\right), \tag{7}$$

where $E_s=\phi_t\cdot T_s$ is normalized transmit energy with $\phi_t=\sum_{n=0}^{N_t-1}\phi_t^{(0,n_t)}$. T_s is the symbol length. The exponential function in Eq. (6) means the phase rotation due to the cyclic delay adding.

The reference signal $X(k)$ is multiplied to frequency-domain received signal and the composite channel gain is estimated. $X(k)$ is given as

$$X(k)=P^*(k)\big/\left|P(k)\right|^2\,, \tag{8}$$

where $(.)^*$ is the complex conjugate operation. The instantaneous composite channel gain estimate is given as

$$\hat{H}_{n_r}^{(v)}(k)=X(k)R_{n_r}(k)\,. \tag{9}$$

The accuracy of the instantaneous composite channel gain estimate is improved by averaging it for N_p blocks.

Average instantaneous composite channel gain estimate are transformed by N_c-point IFFT into the time domain, and the composite channel impulse response estimate $\{\hat{h}_{n_r}(\tau)$; $\tau=0\sim N_c-1\}$ is given. Since each transmit antenna is given a different cyclic delay of an integer multiple of Δ, the channel impulse response associated with N_t transmit antennas do not overlap. By applying the delay time-domain windowing [14] and delay time shift, the channel impulse response estimate between the n_t-th transmit antenna and n_r-th receive antenna is given as

$$\hat{h}_{n_r,n_t}(\tau)=\begin{cases}\hat{h}_{n_r}(\tau+\Delta n_t) & \text{if}\quad 0\leq\tau<\Delta\\ 0 & \text{otherwise}\end{cases}, \tag{10}$$

and then, by applying N_c-point FFT to $\hat{h}_{n_r,n_t}(\tau)$, the channel gain estimate $\hat{H}_{n_r,n_t}(k)$ between n_t-th transmit antenna and n_r-th receive antenna is obtained. Since the impulse response lengths of all transmit antennas are within ΔN_t, (interference+noise) power is estimated by using $\hat{h}_{n_r}(\tau)$ in the delay time-domain where there is no impulse response. By approximating the CCI plus noise as a complex Gaussian variable, (interference+noise) power estimate $\hat{\sigma}_{CCI+noise}^2$ is given as

$$\hat{\sigma}_{CCI+noise}^2=\frac{1}{(N_c-\Delta N_t)}\sum_{\tau=\Delta N_t}^{N_c-1}\left|\hat{h}_{n_r}(\tau)\right|^2\Bigg/\frac{2}{N_c}\sum_{k=0}^{N_c-1}\frac{1}{\left|P(k)\right|^2}\,. \tag{11}$$

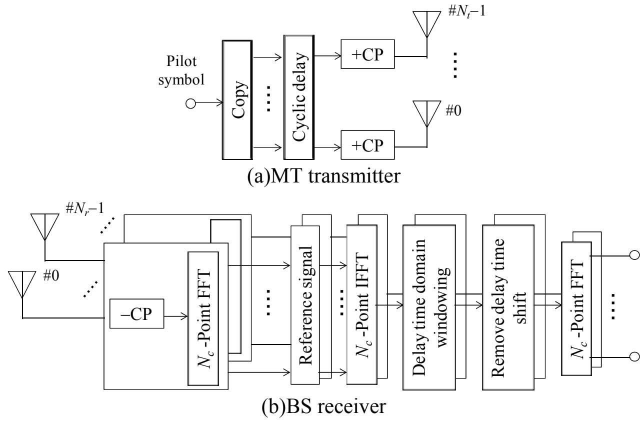

Fig. 4. Transmitter/receiver for CDP-CE.

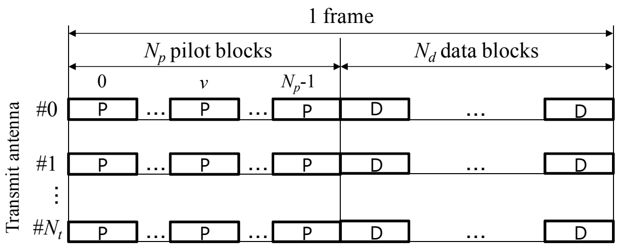

Fig. 5. Frame structure.

B. Adaptive multiplexing order selection

Channel estimate and (interference+noise) power estimate are used to select the multiplexing order Z. In this paper, it is assumed that both transmitter and receiver have 4 antennas. When Z=1, single data stream is transmitted by FD-STTD with N_t=2 because the throughput of FD-STTD with N_t=2 is the best due to the STBC coding rate and the diversity gain [15]. When $Z\geq 2$, Z data streams are transmitted by FD-SDM with N_t=Z. In this paper, Z is selected based on the maximum throughput criterion. First of all, the instantaneous received SINR of each Z(=1~4) is calculated from the channel gain estimate and (interference+noise) power estimate. The instantaneous received SINR of FD-STTD is given as (the derivation is abbreviated)

$$\gamma_0^{\mathrm{STTD}(Z)}\left(\frac{E_s}{N_0},\{\hat{H}_{n_r,n_t}(k)\}\right)\\=\frac{\left|\dfrac{1}{N_c}\sum_{k=0}^{N_c-1}\widetilde{H}_{N_t=2}^{STTD}(k)\right|^2}{\overline{\sigma}_{ISI}^2+\hat{\sigma}_{CCI+noise}^2\cdot\dfrac{1}{N_c}\sum_{n_r=0}^{N_r-1}\sum_{n_t=0}^{N_t-1}\sum_{k=0}^{N_c-1}\left|W_{n_r,n_t}(k)\right|^2}\,, \tag{12}$$

where

$$2\overline{\sigma}_{ISI}^2=\left[\frac{1}{N_c}\sum_{k=0}^{N_c-1}\left|\widetilde{H}_{N_t=2}^{STTD}(k)\right|^2-\left|\frac{1}{N_c}\sum_{k=0}^{N_c-1}\widetilde{H}_{N_t=2}^{STTD}(k)\right|^2\right] \tag{13}$$

with $\widetilde{H}_{N_t=2}^{STTD}(k)$ being the equivalent channel gain of FD-STTD given as

$$\widetilde{H}^{STTD}_{N_t=2}(k)=\sum_{n_r=0}^{N_r-1}\left\{\hat{H}_{n_r,0}(k)W^*_{n_r,0}(k)+\hat{H}^*_{n_r,1}(k)W_{n_r,1}(k)\right\}. \quad (14)$$

$W_{n_r,n_t}(k)$ is the MMSE weight of FD-STTD given as [11]

$$W_{n_r,n_t}(k)=\frac{\hat{H}_{n_r,n_t}(k)}{\sum_{n_r=0}^{N_r-1}\sum_{n_t=0}^{N_t-1}|\hat{H}_{n_r,n_t}(k)|^2+\hat{\sigma}^2_{CCI+noise}}. \quad (15)$$

The instantaneous received SINR of FD-SDM ($Z\geq 2$) at the n_t(=0~Z–1)-th stream is given as (the derivation is omitted for brevity)

$$\gamma^{\mathrm{SDM}(Z)}_{n_t}\left(\frac{E_s}{N_0},\{\hat{H}_{n_r,n_t}(k)\}\right)=\frac{\left|\frac{1}{N_c}\sum_{k=0}^{N_c-1}\widetilde{H}^{SDM}_{n_t,n_t}(k)\right|^2}{\sigma^2_{ISI,n_t}+\sigma^2_{IAI,n_t}+\hat{\sigma}^2_{CCI+noise}\cdot\frac{1}{N_c}\sum_{n_r=0}^{N_r-1}\sum_{k=0}^{N_c-1}\left|\overline{W}_{n_r,n_t}(k)\right|^2}, \quad (16)$$

where

$$2\sigma^2_{ISI,n_t}=\left[\frac{1}{N_c}\sum_{k=0}^{N_c-1}\left|\widetilde{H}^{SDM}_{n_t,n_t}(k)\right|^2-\left|\frac{1}{N_c}\sum_{k=0}^{N_c-1}\widetilde{H}^{SDM}_{n_t,n_t}(k)\right|^2\right] \quad (17)$$

$$2\sigma^2_{IAI,n_t}=\frac{1}{N_c}\sum_{\substack{n'_t=0\\ n'_t\neq n_t}}^{N_t-1}\sum_{k=0}^{N_c-1}\left|\widetilde{H}^{SDM}_{n_t,n'_t}(k)\right|^2, \quad (18)$$

with $\widetilde{H}^{SDM}_{n_t,n_t}(k)$ being the equivalent channel gain of FD-SDM given as

$$\widetilde{H}^{SDM}_{n_t,n'_t}(k)=\sum_{n_r=0}^{N_r-1}\overline{W}_{n_r,n_t}(k)\hat{H}_{n_r,n'_t}(k). \quad (19)$$

$\overline{\mathbf{W}}(k)$ is the $N_t\times N_r$ MMSE weight matrix of FD-SDM having $\overline{W}_{n_r,n_t}(k)$ at the (n_t,n_r)-th component and given as

$$\overline{\mathbf{W}}(k)=\hat{\mathbf{H}}^H(k)\left(\hat{\mathbf{H}}(k)\hat{\mathbf{H}}^H(k)+\hat{\sigma}^2_{CCI+noise}\mathbf{E}\right)^{-1}, \quad (20)$$

where $\mathbf{E}$ is the $N_r\times N_r$ identify matrix. $(.)^H$ is the Hermitian transpose operation. $\hat{\mathbf{H}}(k)$ is the $N_r\times N_t$ frequency-domain channel gain matrix in the k-th frequency expressed as

$$\hat{\mathbf{H}}(k)=\begin{bmatrix}\hat{H}_{0,0}(k) & \cdots & \hat{H}_{0,N_t-1}(k)\\ \vdots & \ddots & \vdots\\ \hat{H}_{N_r-1,0}(k) & \cdots & \hat{H}_{N_r-1,N_t-1}(k)\end{bmatrix}. \quad (21)$$

The conditional bit error rate (BER) is calculated from the instantaneous received SINR. The conditional BER of QPSK modulation is given as [12]

$$p^{(Z)}_{b,QPSK}\left(\frac{E_s}{N_0},\{\hat{H}_{n_r,n_t}(k)\}\right)=\frac{1}{2Z}\sum_{n_t=0}^{Z-1}\mathrm{erfc}\left[\sqrt{\frac{1}{4}\gamma^{(Z)}_{n_t}\left(\frac{E_s}{N_0},\{\hat{H}_{n_r,n_t}(k)\}\right)}\right], \quad (22)$$

where $\mathrm{erfc}[x]=(2/\pi)\int_x^\infty \exp(-t^2)dt$ is complementary error function.

The instantaneous packet error rate (PER) is calculated as

$$\mathrm{PER}^{(Z)}=1-\left\{1-p^{(Z)}_{b,QPSK}\left(\frac{E_s}{N_0},\{\hat{H}_{n_r,n_t}(k)\}\right)\right\}^K, \quad (23)$$

where K is the packet size. The theoretical instantaneous throughput is calculated by using the instantaneous PER as

$$\eta^{(Z)}\equiv\frac{Z\times\log_2 M\times(1-\mathrm{PER}^{(Z)})}{F}\times\frac{N_c}{N_c+N_g}\times\frac{N_d}{N_d+N_p}, \quad (24)$$

where M is the modulation level (when QPSK is used, M=4). The multiplexing order having the highest throughput is selected as

$$\overline{Z}=\arg\max_Z \eta^{(Z)}. \quad (25)$$

The selected multiplexing order is fed back to the transmitter. FD-STTD is used when $\overline{Z}=1$ and FD-SDM is used when $\overline{Z}\geq 2$. In this paper, the ideal $\overline{Z}$ feedback is assumed.

IV. COMPUTER SIMULATION RESULTS

The throughput performance is evaluated by computer simulation. Computer simulation condition is summarized in Table I. A frequency-selective block Rayleigh fading channel having a symbol-spaced L=8-path uniform power delay profile is assumed. The fading between each transmit and receive antenna has no correlation. QPSK modulation is assumed. Both MT and BS have 4 antennas. Z=1, 2, 3, and 4 is selected based on the maximum throughput criterion. The cluster size F is set to 7. 10% and 90% outage throughputs (10% and 90% value of cumulative distribution function of throughput) are evaluated.

First of all, ideal channel estimation is assumed. Fig. 6 plots the throughputs achievable with MIMO adaptive multiplexing order selecting transmission and MIMO fixed multiplexing order transmission as a function of the normalized total transmit E_s/N_0. It can be seen from Fig. 6 that the MIMO adaptive multiplexing order selecting transmission achieves the best throughput performance. For 10% outage throughput (i.e., throughput near the cell edge), the proposed MIMO adaptive multiplexing order selecting transmission can achieve the highest throughput by selecting Z=1 (i.e., FD-STTD) because the impact of CCI is strong. On the other hand, for 90% outage throughput (i.e., throughput near the cell center), the proposed MIMO adaptive multiplexing order selecting transmission can achieve the highest throughput by selecting the multiplexing order according to the received SINR. From the results, it is shown that MIMO adaptive multiplexing order selecting transmission can achieve higher throughput than the fixed MIMO transmission in various propagation environments.

In the next, channel estimation by CDP-CE is assumed. Fig. 7 plots the throughput achievable with MIMO adaptive multiplexing order selecting transmission using CDP-CE. Fig. 7 (a) plots the 10% outage throughput and Fig. 7 (b) plots the 90% outage throughput. From Fig. 7 (a), 10% outage throughput with N_p=1 gets worse than those with other N_p. When N_p=1, the channel estimate quality becomes low because the channel and (interference+noise) power averaging are not enough. On the other hand, the channel estimate quality gets better as N_p increases, and hence, the throughput is improved in low normalized total transmit E_s/N_0 area. But peak throughput degrades in high normalized total transmit E_s/N_0 area because the impact of pilot insertion loss is bigger than that of estimation quality improvement. From Fig. 7 (b), 90% outage throughput is improved with $N_p\geq 2$ in low normalized total transmit E_s/N_0 area. However, peak throughput degrades in high normalized total transmit E_s/N_0 area and the pilot insertion loss becomes bigger as N_p increases. The same reason can be applied to the case of 10% outage throughput. From these results, N_p=2 is enough to get a good 10% and 90% outage throughput performance.

Table I. Computer simulation condition.

Transmitter	Data modulation	QPSK
	No. of users per cell	U=1
	No. of FFT points	N_c=64
	Length of CP	N_g=8
	No. of pilot blocks	N_p=1,2,3,4
	No. of data blocks	N_d=12
	Packet size	K=1536bits
	Pilot sequence	Chu sequence [16]
	No. of transmit antennas	N_t=2,3,4
Channel model	Fading	Frequency-selective Block Rayleigh
	No. of paths	L=8
	Power delay profile	Uniform
	Time delay	$\tau^{(l)}_{n_r,n_t}=lT_s$, l=0~L–1
	Path-loss exponent	α=3.5
	Standard deviation of shadowing loss	σ_s=7.0dB
	Cluster size	F=7
Receiver	No. of receive antennas	N_r=4
	Channel estimation	Ideal, CDP-CE

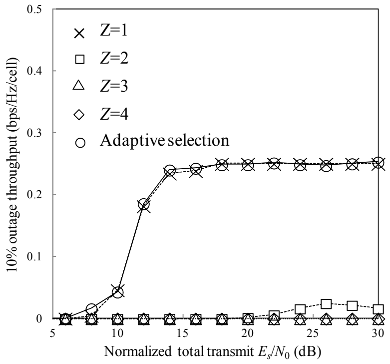

(a)10% outage throughput

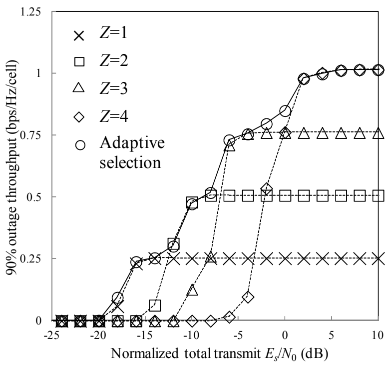

(b)90% outage throughput

Fig. 6. Throughput performance with ideal channel estimation.

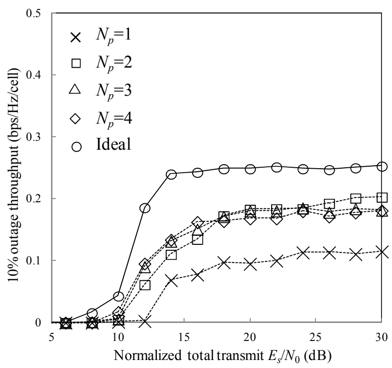

(a)10% outage throughput

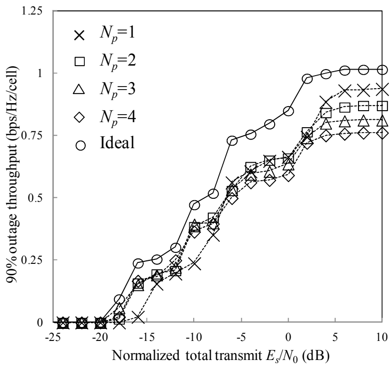

(b)90% outage throughput

Fig. 7. Throughput performance with CDP-CE.

V. Conclusion

In this paper, we proposed an adaptive multiplexing order selection for SC-MIMO with FDE using practical MIMO channel estimation called CDP-CE and evaluated the uplink throughput by computer simulation in a multi-cell environment. The computer simulation showed that the insertion of only two pilot blocks per flame is sufficient for CDP-CE and that the proposed adaptive multiplexing order selection achieves always higher throughput than the fixed multiplexing order case.

References

[1] A. Goldsmith, *Wireless Communications*, Cambridge University Press, 2005.

[2] E. Biglieri, R. Calderbank, A. Constantinides, A. Goldsmith, A. Paulraj, and H. V. Poor, *MIMO Wireless Communications*, Cambridge University Press, 2007.

[3] L. Zheng and D. N. C. Tse, “Diversity and multiplexing: a fundamental tradeoff in multiple-antenna channels,” IEEE Trans. Inf. Theory, vol. 49, no. 5, pp. 1073-1096, May 2003

[4] S. M. Alamouti, “A simple transmit diversity technique for wireless communication,” IEEE J. Select. Areas. Commun, vol. 16, no. 8, pp. 1451-1458, Oct. 1998.

[5] A. Van Zelst, R. Van Nee, and G. Awater, “Space division multiplexing for OFDM systems,” Proc. 2000 IEEE Veh. Tech. Conf.(VTC), vol.2, pp.1070-1074, May 2000.

[6] R. W. Heath and Jr. A J Paulraj, “Switching between Diversity And Diversity in MIMO Systems,” IEEE Trans. Commun., vol. 53, no. 6, pp. 962-968, Jun. 2005.

[7] K. Tadakamalla and K. Kokkula, “Switching in MIMO-frequency selective channels,” International Journal of Communication and Electrical Engineering, vol. 2, no. 4, pp. 613-616, Aug. 2005.

[8] C. Kim and J. Lee, “Dynamic rate-adaptive MIMO mode switching between spatial multiplexing and diversity,” EURASIP Journal on Wireless Communications and Networking, 2012:238, doi:10.1186/1687-1499-2012-238.

[9] D. Falconer, S. L. Ariyavisitakul, A. Benyamin-Seeyar, and B. Edison, “Frequency domain equalization for single-carrier broadband wireless systems,” IEEE Commun. Mag., vol.40, no. 4, pp. 58-66. Apr. 2002.

[10] F. Adachi, H. Tomeba, and K. Takeda, “Introduction of frequency-domain signal processing to broadband single-carrier transmissions in a wireless channel,” IEICE Trans. Commun., vol.E92-B, no.9, pp. 2789-2808, Sept. 2009.

[11] K. Takeda, T. Itagaki, and F. Adachi, “Application of space-time transmit diversity to single carrier transmission with frequency-domain equalization and receive antenna diversity in a frequency-selective fading channel,” IEE Proc.-Commun., vol. 151, no. 6, pp. 627-632, Dec. 2004.

[12] J. G. Proakis and M. Salehi, *Digital communications*, 5th edition, McGraw-Hill, 2008.

[13] T. Fujimori, Kazuki Takeda, K. Ozaki, A. Nakajima, and F. Adachi, “Channel estimation using cyclic delay pilot for SC-MIMO multiplexing,” IEICE Trans. Commun., vol.E91-B, no. 9, pp.2925-2932, Sept. 2008.

[14] J. J. de Beek, O. Edfors, M. Sandell, S. K. Wilson, and P. O. Borjesson, “On channel estimation in OFDM systems,” Proc. IEEE 45th Vehicular Technology Conference (VTC), vol.2, pp.815-819, July 1995.

[15] H. Tomeba and F. Adachi, “Throughput performance of MC-CDMA HARQ using space-time block coded-joint transmit/receive antenna diversity,” Proc. IEEE 70th Vehicular Technology Conference (VTC2009-Fall), Anchorage, Alaska, USA, Sept. 2009.

[16] D. C. Chu, “Polyphase codes with good periodic correlation properties,” IEEE Trans. Inf. Theory. vol. 5, no. 7, pp. 531-532, July 1972.